

1 **Electronic Supplementary Information**

2 **MOF-Derived Hollow SiO_x Nanoparticles Wrapped in 3D**

3 **Porous Nitrogen-doped Graphene Aerogel and their Superior**

4 **Performance as the Anode for Lithium-ion Batteries**

5 *Chenfeng Guo*, Ying Xie, Kai Pan and LiLi*

6 *School of Chemistry and Materials Science, Key Laboratory of Functional Inorganic*

7 *Material Chemistry, Ministry of Education, Heilongjiang University, Harbin 150080,*

8 *People's Republic of China*

9 * Corresponding author: Chenfeng Guo

10 E-mail: chenfengguo@hlju.edu.cn (Dr. Chenfeng Guo)

11 Tel: +86-451-86608545;

12

13

14

15

16

17

18

19

20

21

22

23

24

25

26

27

28

29

30

1 Experimental Section

2 Materials synthesis

3 *MOF template synthesis of hollow SiO_x nanoparticles:*

4 Hollow SiO₂ nanoparticles were fabricated with MOF (zeolitic imidazolate framework-8 (ZIF-8)) as both
5 the precursor and the self-sacrificing template.^[1] Briefly, solution of cetyltrimethylammonium bromide
6 (CTAB), Zn(NO₃)₂ · 6H₂O and 2-methylimidazole (Hmim) were mixed together in fixed proportions at
7 room temperature, and then reacted using methanol as solvent without stirring for 24 h. The ZIF-8
8 nanoparticles were obtained after centrifugation, washing and drying under vacuum. The core-shell
9 ZIF-8@SiO₂ microstructure were prepared through a versatile Stöber sol-gel method.^[2, 3] Then the
10 hollow SiO₂ nanoparticles were obtained with the hydrothermal treatment of 24 h with hydrochloric
11 acid, and the obtained hollow SiO₂ nanoparticles powders were annealed at 1000 °C for 2 h in reductive
12 atmosphere of hydrogen (5%) and balanced by argon (5% H₂ and 95% Argon) to produce hollow SiO_x
13 nanoparticles.^[4] The aminopropyl trimethoxysilane (APS)-modified hollow SiO_x nanoparticles were
14 prepared with a surface modification method.^[5]

15 *Fabrication of hollow SiO_x nanoparticles @N-doped graphene aerogel (HSiO_x@N-GA):*

16 Graphite oxide (GO) was synthesized with the modified Hummers method as previously reported.^[6]
17 HSiO_x@N-GA was synthesized with a modified process.^[7] Typically, solution of GO (1 mg ml⁻¹) and
18 solution of APS-modified hollow SiO_x nanoparticles (5 mg ml⁻¹) were homogeneously mixed under
19 sonication (20 min), the hollow SiO_x nanoparticles@GO was obtained after centrifugation and rinsing
20 with deionized water for several times. In the controllable experiment, the weight percent of hollow
21 SiO_x nanoparticles was typically kept at 84%. Subsequently, hollow SiO_x nanoparticles@GO was
22 homogeneously dispersed in urea (100 mg ml⁻¹) aqueous solution, then transferred into a Teflon-lined
23 stainless steel autoclave, and reacted at 150 °C for 6 h. After the autoclave was naturally cooled to room
24 temperature, the resulting N-doped graphene hydrogel embedded with hollow SiO_x nanoparticles
25 (hollow SiO_x nanoparticles@N-doped graphene hydrogel) were rinsed with deionized water for several
26 times, and then freeze-dried. Finally, for completing the reduction process of hollow SiO_x nanoparticles
27 and bits of residual GO, the product was annealed at 500 °C for 2 h in reductive atmosphere (5% H₂ and
28 95% Argon) to generate 3D HSiO_x@N-GA. For comparison, hollow SiO_x nanoparticles@GA (HSiO_x@GA)
29 were fabricated by the same method with the preparation process of HSiO_x@N-GA without adding
30 urea. N-GA and GA were fabricated by assembly of GO by using the same hydrothermal method in the
31 presence and without adding urea, respectively.

32 Materials characterization

33 The collected products were characterized by using powder X-ray diffraction (XRD) on a Rigaku
34 diffractometer with Cu K α radiation. X-ray photoelectron spectroscopy (XPS, Kratos Axis ULTRA) was
35 performed to analyze the chemical compositions of the synthesized samples. N₂ adsorption and
36 desorption isotherms at 77K were measured by using a Tristar II 3020 instrument, and the specific
37 surface area was measured by utilizing the Brunauer-Emmett-Teller (BET) method. The pore diameter
38 and pore size distribution were calculated by the Barrett-Joyner-Halenda (BJH) model. Raman
39 measurements were performed at room temperature by using Thermo-Fischer Almega dispersive
40 Raman instrument with the excitation wavelength of 633 nm. Fourier transform infrared (FTIR) spectra
41 were recorded with a Nicolet 5700 FTIR spectrometer. Thermal gravimetric analysis (TGA, Mettler
42 Toledo TGA/DSC1 STARe System) was measured with a 10 °C min⁻¹ heating rate in air flow from room

1 temperature up to 800 °C. A four-probe conductivity test metre was used to measure the electronic
2 conductivity of samples at room temperature (SB120; San Feng). The morphology and microstructure
3 of the samples were obtained from field-emission scanning electron microscope (FESEM, Hitachi S-
4 4800), transmission electron microscope (TEM, JEOL1010) and high-resolution (HRTEM, FEI Tecnai20).
5 The TEM and HRTEM samples were disposed by dispersion in ethanol with sonication of scraped
6 nanoparticles, and dropping onto Cu grids with carbon-coating. A high precision electronic balance
7 (XP105DR, Mettler Toledo) was utilized to tip the scale at all the materials.

8 **Electrochemical Measurement**

9 ***Fabrication of Electrodes and Coin Cells:***

10 Electrodes were fabricated by mixing the as-obtained HSiO_x@N-GA as the active material,
11 polyvinylidene fluoride (PVDF) as binder, N-methyl-2-pyrrolidone (NMP) as solvent, and carbon black
12 as conductor with a mass ratio of 80:10:10 to form a mixture (slurry). The resulting slurries were pasted
13 onto Cu foil (as a current collector), after drying at 75 °C for 12 h in vacuum oven and compressing at a
14 given pressure, the Cu foil was cut into disks with diameter of 1.5 cm with average loading masses of
15 *ca.* 1 mg/cm². The CR2032-type half-cells that were assembled in an argon-filled glove box with
16 controlling the contents of oxygen and moisture under 1 ppm, and 1 M of LiPF₆ in ethylene carbonate
17 (EC)/dimethyl carbonate (DMC)/diethyl carbonate (DEC) solvent (1:1:1 vol/vol/vol) was utilized as an
18 electrolyte, with Celgard 2500 (polypropylene) as separator, active material as anode and metal lithium
19 disks as cathode.

20 ***Electrochemical Characterization:***

21 The galvanostatically discharged and charged measurements of the cells were tested on a Land
22 (CT2001A) system over a voltage range of 0.01-1.5 V (vs. Li/Li⁺) at room temperature. Noting that “n C”
23 means that the discharge/charge current is set up to attain the nominal capacity in “1/n” hours. For
24 HSiO_x@N-GA electrode, the weight of HSiO_x@N-GA in the working electrode was applied to judge the
25 specific discharge capacity of the cell, which was showed in mAhg⁻¹ of HSiO_x@N-GA. On the basis of the
26 equation described below, we could calculate a theoretical capacity (Q) of the hypothetical mixture of
27 HSiO_x@N-GA, as follows:

$$\begin{aligned} 28 \quad Q_{\text{theoretical}} &= Q_{\text{hollow SiO}_x \text{ nanoparticles}} \times \text{mass percentage of hollow SiO}_x \text{ nanoparticles} + Q_{\text{N-GA}} \times \text{mass} \\ 29 \quad &\quad \text{percentage of N-GA} \\ 30 \quad &= 2400 \times 83.74\% + 372 \times 16.26\% = 2070.72 \text{ mAhg}^{-1} \end{aligned}$$

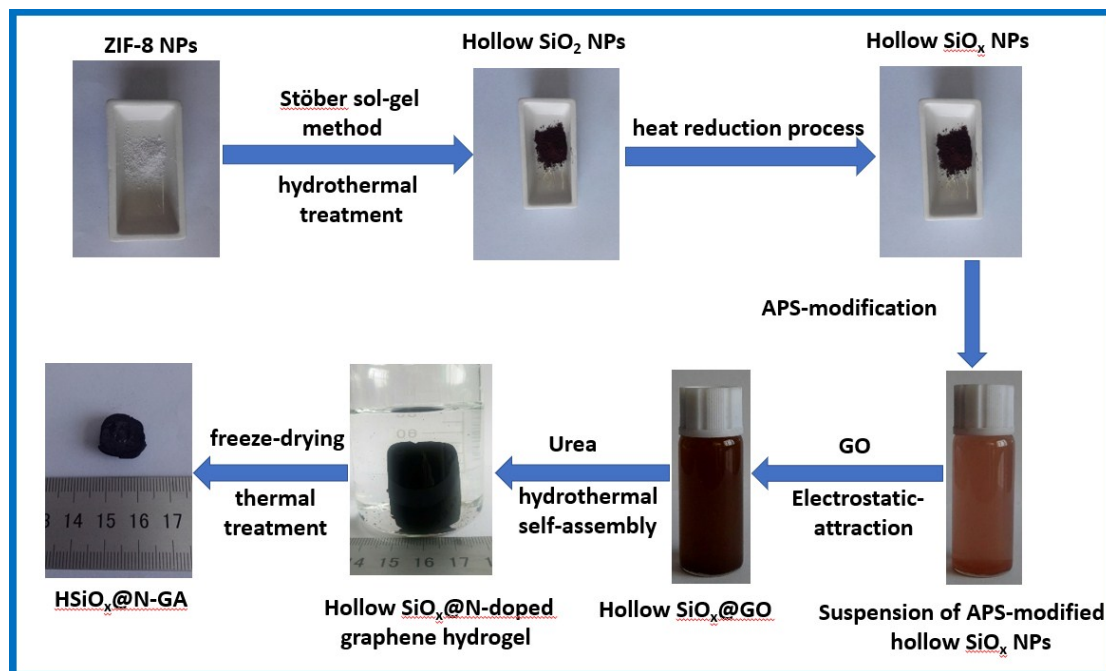
31 (The theoretical capacity (Q) of SiO_x was calculated on the basis of theoretical capacity of SiO previously
32 reported,^[8] owing to the average valence state of Si in HSiO_x@N-GA is calculated to be *ca.* 2.11, the
33 value that is on the verge of the theoretical valence state of Si (2.0) in SiO.)

34 Cyclic voltammetry (CV) curves were collected by a CHI660C electrochemistry workstation at 0.1 mV·s⁻¹
35 between 0.01-3.0 V (vs. Li/Li⁺). Electrochemical impedance spectroscopy (EIS) of the as-prepared
36 anodes were measured on a PARSTAT 2273 electrochemical station over a frequency range of 10 000-
37 0.1 Hz with an amplitude of 5 mV. Recurrence of the electrochemical data was verified by repeating the
38 experiments until obtaining at least another anode of the same specimen.

39
40
41
42
43
44

1

2 **S1. Photograph illustration of the preparation procedure of $\text{HSiO}_x\text{@N-GA}$.**



3

4 **Fig. S1†** The photograph illustration of the preparation process of $\text{HSiO}_x\text{@N-GA}$. Hollow SiO_x
5 nanoparticles were synthesized with method of MOF-templet inducing, including fabrication of ZIF-8,
6 Stöber sol-gel synthesis, hydrothermal treatment and heat reduction process. Hollow $\text{SiO}_x\text{@GO}$, which
7 existed in the form of stable and uniform suspension, was obtained by the electrostatic-attraction
8 between APS-modified hollow SiO_x nanoparticles and GO. Hollow $\text{SiO}_x\text{@N-doped}$ graphene hydrogel
9 was prepared by hydrothermal self-assembly with urea. After the freeze-drying and thermal treatment
10 process, a monolithic hybrid aerogel ($\text{HSiO}_x\text{@N-GA}$) was obtained.

11

12

13

14

15

16

17

18

19

20

21

22

23

24

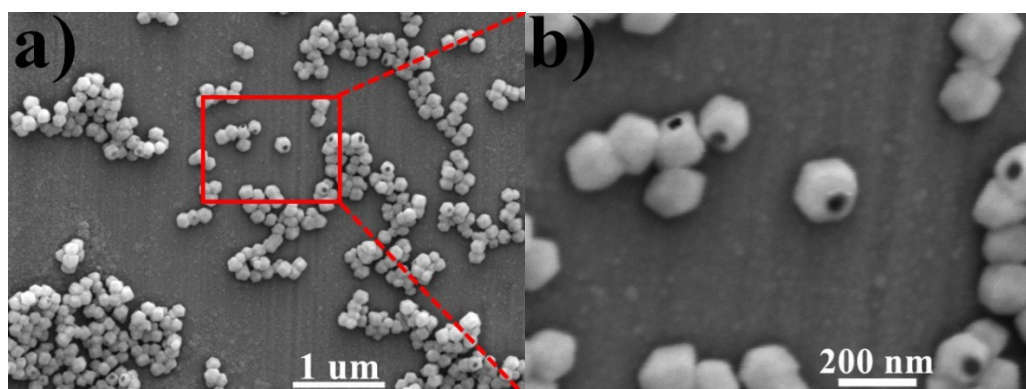
25

26

1

2 **S2. Morphology information of the as-prepared hollow SiO_x nanoparticles**

3



4 **Fig. S2†** (a) Low-magnification, (b) high-magnification SEM images of the as-prepared hollow SiO_x
5 nanoparticles, showing hollow SiO_x nanoparticles exhibited the uniform sodalite zeolite-type structure-
6 rhombic dodecahedral shape, as well as obvious irregular aggregation between hollow SiO_x
7 nanoparticles, and average size of hollow SiO_x nanoparticles was ranged 100-160 nm; (b) is
8 corresponding to the red-rectangle area in (a).

9

10

11

12

13

14

15

16

17

18

19

20

21

22

23

24

25

26

27

28

29

30

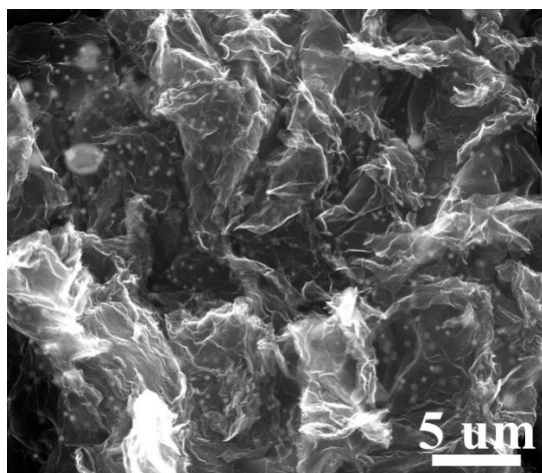
31

32

33

1

2 **S3. Morphology information of the as-prepared HSiO_x@N-GA at low magnification**



3

4 **Fig. S3†** SEM images of HSiO_x@N-GA at low magnification, showing hollow SiO_x nanoparticles were
5 wrapped in the interior and surface of porous N-GA network.

6

7

8

9

10

11

12

13

14

15

16

17

18

19

20

21

22

23

24

25

26

27

28

29

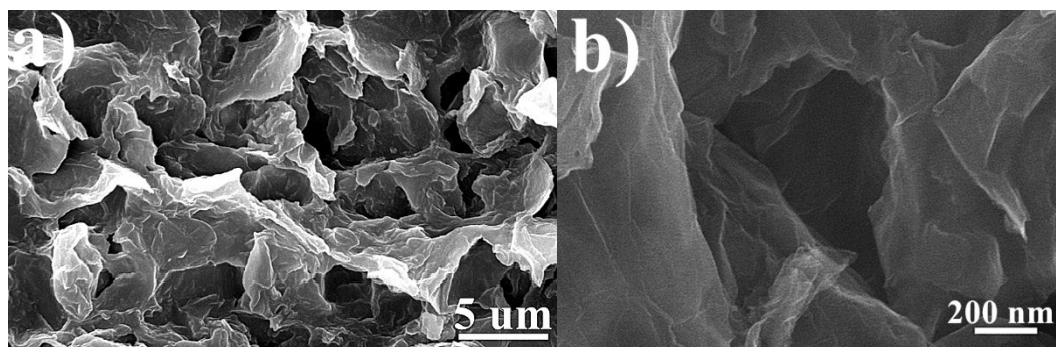
30

31

1

2 **S4. Morphology information of the as-prepared N-GA**

3



4 **Fig. S4†** SEM images of N-GA, showing fully interconnected, porous 3D graphene frameworks with
5 randomly opened macro-/mesoporous structure.

6

7

8

9

10

11

12

13

14

15

16

17

18

19

20

21

22

23

24

25

26

27

28

29

30

31

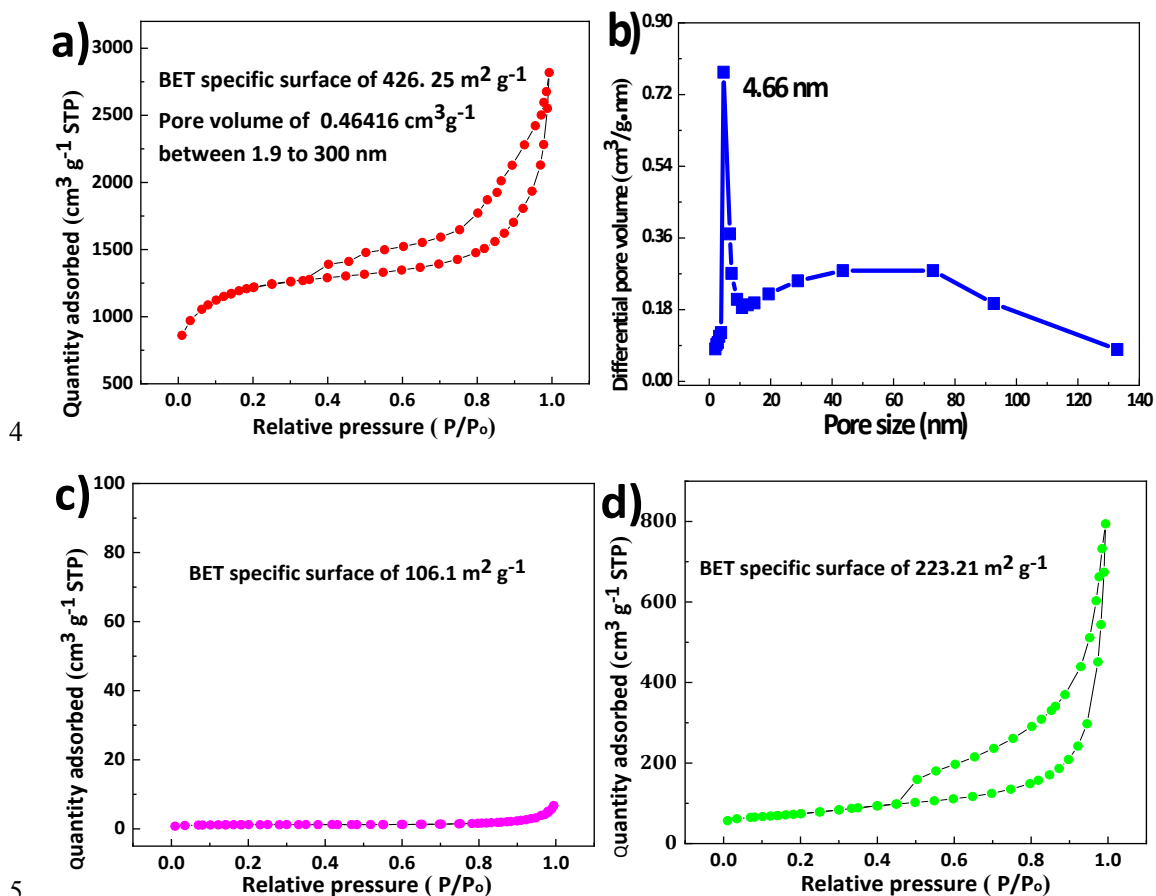
32

33

34

35

1
2 **S5. Nitrogen isothermal adsorption-desorption measurement of HSiO_x@N-GA,**
3 **hollow SiO_x nanoparticles and N-GA.**

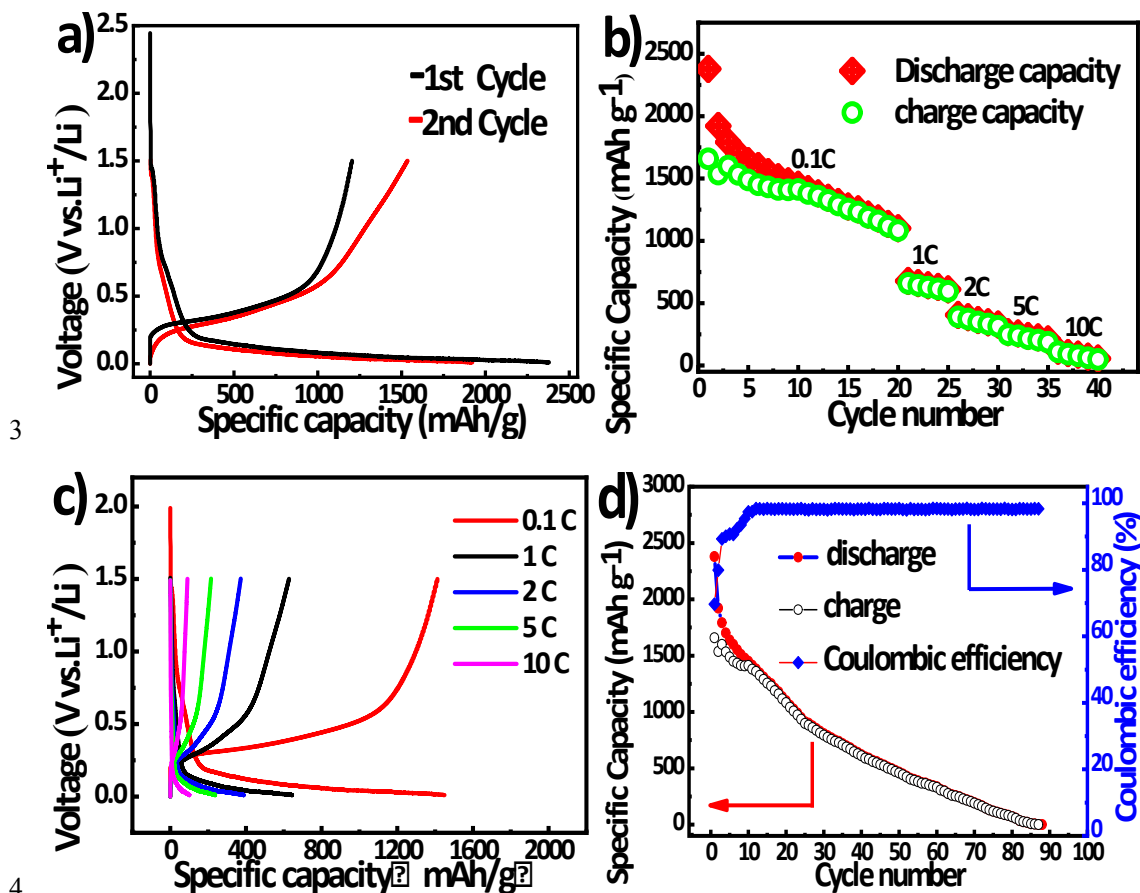


6 **Fig. S5†** (a) Nitrogen adsorption-desorption isotherm plot of HSiO_x@N-GA at 77 K; (b) BJH adsorption
7 pore size distribution profiles of HSiO_x@N-GA; (c and d) Nitrogen adsorption-desorption isotherm plots
8 of hollow SiO_x nanoparticles and N-GA at 77 K.

9
10
11
12
13
14
15
16
17
18
19
20
21
22
23

1

2 **S6. Electrochemical performance of hollow SiO_x nanoparticles.**



5 **Fig. S6†** Electrochemical properties of hollow SiO_x nanoparticles: (a) discharge and charge profiles for
6 the initial two cycles at 0.1 C. The first discharge and charge capacities are 2380 and 1204 mA h g⁻¹ with
7 an initial Coulombic efficiency of 50.6%. The capacity is based on total anode mass of hollow SiO_x
8 nanoparticles. (b) rate performance cycled from 0.1 C to 10 C. (c) discharge and charge profiles at
9 current rates ranging from 0.1 C to 10 C and (d) cycling performance at 0.1 C and Coulombic efficiency.
10 Hollow SiO_x nanoparticles anode was un-rechargeable under a current rate of 0.1C after 87 cycles,
11 suggesting an inferior cycling performance.

12

13

14

15

16

17

18

19

20

21

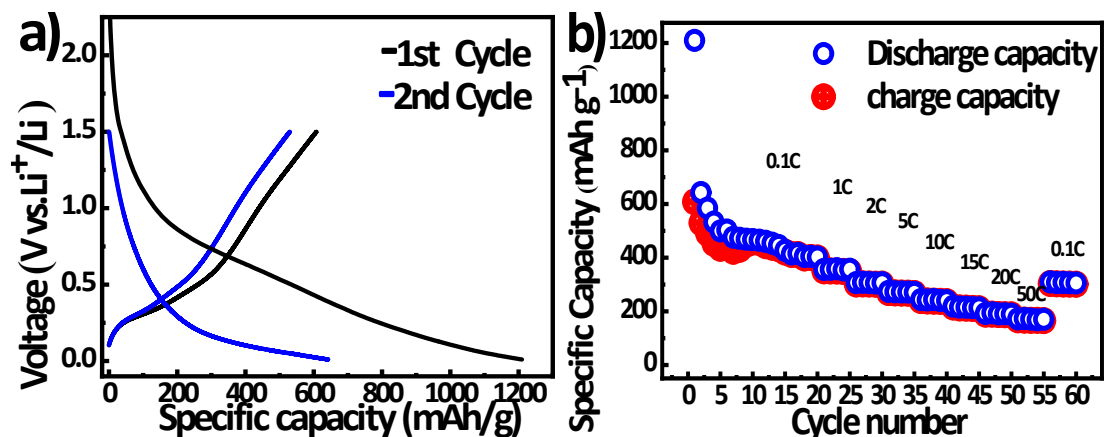
22

23

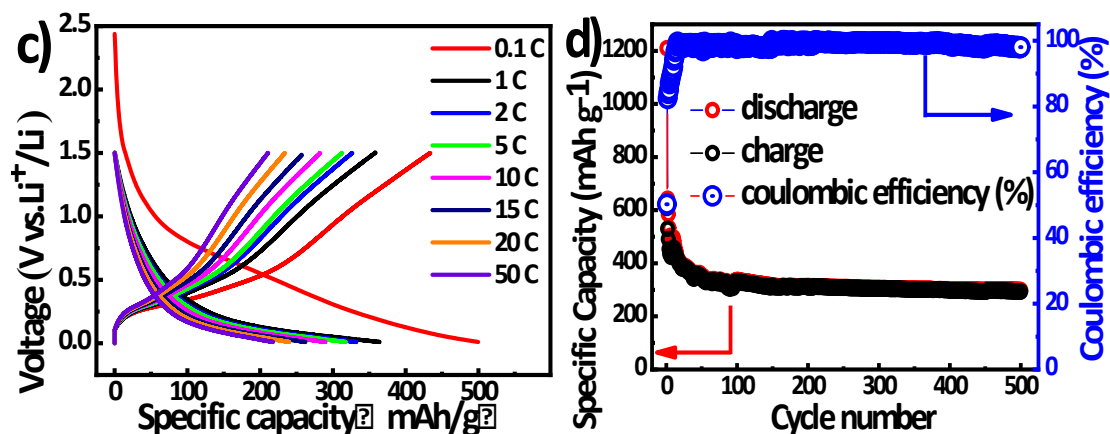
1

2 **S7. Electrochemical performance of N-GA.**

3



3



4

5 **Fig. S7†** Electrochemical properties of N-GA: (a) discharge and charge profiles for the initial two cycles
6 at 0.1 C. The first discharge and charge capacities are 1209.5 and 608.1 mA h g⁻¹ with an initial
7 Coulombic efficiency of 50.27%. The capacity is based on total anode mass of N-GA. (b) rate
8 performance cycled from 0.1 C to 50 C. (c) discharge and charge profiles at current rates ranging from
9 0.1 C to 50 C and (d) cycling performance at 0.1 C and Coulombic efficiency. N-GA exhibits a charge
10 capacity of 293 mA h g⁻¹ under a current rate of 0.1C after 500 cycles, suggesting a common cycling
11 stability.

12

13

14

15

16

17

18

19

20

21

22

23

1
2

3 **References:**

- 4 [1] Liu He, Lu Li, Lingyu Zhang, Shuangxi Xing, Tingting Wang, Guangzhe Li, Xiaotong Wu, Zhongmin Su
5 and Chungang Wang, *CrystEngComm*, 2014, **16**, 6534.
- 6 [2] W. Li, Y. H. Deng, Z. X. Wu, X. F. Qian, J. P. Yang, Y. Wang, D. Gu, F. Zhang, B. Tu and D. Y. Zhao, *J.*
7 *Am.Chem. Soc.*, 2011, **133**, 15830.
- 8 [3] X. Q. Zhang, H. Ren, T. T. Wang, L. Y. Zhang, L. Li, C. G. Wang and Z. M. Su, *J. Mater. Chem.*, 2012, **22**,
9 13380.
- 10 [4] SangKyu Lee, SeungMin Oh, Eunjun Park, Bruno Scrosati, Jusef Hassoun, MinSik Park, YoungJun Kim,
11 Hansu Kim, IliasBelharouak and YangKook Sun, *Nano Lett.* 2015, **15**, 2863-2868.
- 12 [5] W.B. Luo, S.L. Chou, Y.C. Zhai and H.K. Liu, *J. Mater. Chem. A*, 2014, **2**, 4927-4931.
- 13 [6] Z. Xiong, L. L. Zhang, J. Ma and X. S. Zhao, *Chem. Commun.*, 2010, **46**, 6099-6101.
- 14 [7] W. Wei, S. Yang, H. Zhou, I. Lieberwirth, X. Feng and K. Müllen, *Adv. Mater.*, 2013, **25**, 2909-2914.
- 15 [8] YaJun Chao, Xianxia Yuan and ZiFeng Ma, *Electrochimica Acta.*, 2008, **53**, 3468-3473.